Bioorganic & Medicinal Chemistry 18 (2010) 8618–8629

Contents lists available at ScienceDirect

Bioorganic & Medicinal Chemistry

journal homepage: www.elsevier.com/locate/bmc

Structure based optimization of chromen-based TNF-α converting enzyme (TACE) inhibitors on S1′ pocket and their quantitative structure–activity relationship (QSAR) study

Jee Sun Yang [a], Kwangwoo Chun [a,b], Jung Eun Park [a], Misun Cho [a], Jeongjea Seo [a], Doona Song [a], Hongchul Yoon [a], Chun-Ho Park [b], Bo-Young Joe [b], Jong-Hee Choi [b], Myung-Hwa Kim [b,*], Gyoonhee Han [a,c,*]

[a] Translational Research Center for Protein Function Control, Department of Biotechnology, Yonsei University, Seodaemun-gu, Seoul 120-749, Republic of Korea
[b] Drug Discovery Laboratory, R&D Center, Jeil Pharmaceutical Co., Ltd, 117-1, Keungok-Ri, Baekam-Myun, Cheoin-Gu, Yongin-City, Kyunggi-Do 449-861, Republic of Korea
[c] Department of Integrated OMICS for Biomedical Sciences (WCU Program), Yonsei University, Seodaemun-gu, Seoul 120-749, Republic of Korea

ARTICLE INFO

Article history:
Received 4 August 2010
Revised 3 October 2010
Accepted 5 October 2010

Keywords:
Chromen-based TACE inhibitors
Optimization
Docking
Quantitative structure–activity relationship
Genetic function approximation

ABSTRACT

A series of coumarin based TACE inhibitors were designed to bind in S1′ pocket of TACE enzyme based on their docking study. Twelve analogues were synthesized and most of compounds were active in vitro TACE enzyme inhibition as well as cellular TNF-α inhibition. Among these, **15l** effectively inhibited the production of serum TNF-α by oral administration at a dose of 30 mg/kg. Compound **15l** also showed a good oral bioavailability at 42% and effectively inhibited paw edema in rat carrageenan model. Quantitative structure–activity relationship (QSAR) study using genetic function approximation technique (GFA) and docking study were performed to confirm the series of coumarin core TACE inhibitors. QSAR model have been evaluated internally and externally using test set prediction. Through docking study of each molecule, it is validated that the electrostatic descriptors from the QSAR equation could explain the importance of S1′ pocket and the TACE inhibitory activity well.

© 2010 Elsevier Ltd. All rights reserved.

1. Introduction

Tumor necrosis factor-α (TNF-α) is one of the major pro-inflammatory cytokines produced by activated macrophages and monocytes.[1,2] The overproduction of TNF-α is responsible for many autoimmune disorders such as rheumatoid arthritis, psoriasis, Crohn's disease,[3] ulcerative colitis,[4] diabetes,[5] multiple sclerosis,[6] atherosclerosis,[7] and stroke.[8] The clinical success of anti-TNF-α biologics for treating inflammatory diseases, such as TNF-α antibody Remicade® (infliximab) and Humira® (adalimumab), and the soluble TNF receptor Enbrel® (etanercept), have suggested that inhibition of TNF-α would be a valid approach for an effective treatment of rheumatoid arthritis, Crohn's disease, and psoriasis.[9–11] Despite the success of the biological agents and discovery of a cost-effective, precisely controllable, orally active, and selective small molecule of anti-TNF-α would be desirable.[4] Inhibition of TNF-α function can be targeted at two different levels; one is inhibition of pro-TNF-α processing by inhibiting TNF-α converting enzyme (TACE) to reduce the amount of active and soluble TNF-α, and the other is inhibition of pro-TNF-α synthesis by blocking nuclear factor (NF)-κB activation cascade.[12] The orally bioavailable small molecule TACE inhibitors could be considered as the effective treatment for rheumatoid arthritis and other inflammatory diseases by reducing the levels of soluble-TNF-α.[4,13]

As the catalytic site of TACE and matrix metalloproteinase (MMP) has high amino acid sequence similarity, the early MMP inhibitors, such as marimastat, prinomastat, and CGS27023A showed TACE inhibitory activity.[14] But the MMP inhibitors showed musculoskeletal side effects and failed in clinical trials for unknown reason.[15] Though the reason for the side effect is obscure, some researchers reported that the inhibition of MMP-1 and/or MMP-14 causes toxicity.[16] Hence, developing selective TACE inhibitors or dual TACE and MMP inhibitors without MMP-1 inhibition are desirable.

On our ongoing discovery program of potent TACE inhibitors,[17] a series of chromen-base analogues were prepared and evaluated for their in vitro potencies.[18] Among these inhibitors, the most active compound, **1a** (Fig. 1) has IC_{50} value of 3 nM for TACE inhibition and found 347 time more selective to TACE over MMP-2 with no inhibition of MMP-9 at 10 μM. α-Methylated analogue (**1a**) and benzylated one (**1b**) show 20 and 12 times increase in the inhibitory potency to TACE compared to the non-alkylated analogue, respectively. Attaining further understanding on the relationship between the structure and biological activity based on quantitative structure–activity relationship (QSAR) is useful tool for design of more potent inhibitors.

* Corresponding authors. Tel.: +82 31 332 4457; fax: +82 31 333 0337 (M.-H.K.); tel.: +82 2 21232882; fax: +82 2 3627265 (G.H.).
E-mail addresses: mhkim@jeilpharm.co.kr (M.-H. Kim), gyoonhee@yonsei.ac.kr (G. Han).

0968-0896/$ - see front matter © 2010 Elsevier Ltd. All rights reserved.
doi:10.1016/j.bmc.2010.10.006

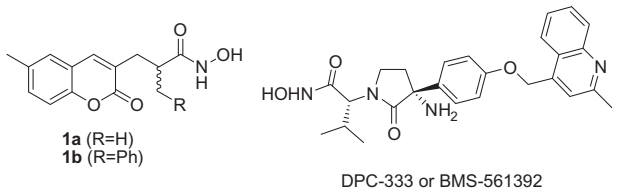

Figure 1. (a) Structure of chromen-based TACE Inhibitor (**1a**, **b**) and DPC-333.

In this paper, we will report design and synthesis of the chromen-core TACE inhibitors for the optimization of S1′ pocket modification, and QSAR study using genetic function approximation (GFA) technique. Furthermore we have docked α-substituted chromen-based analogues into the TACE enzyme to attain a clear percept of the structure–activity relationship of this series of compounds.

2. Methods

2.1. Synthesis

The series of α-substituted chromen-based analogues were prepared using the Wittig coupling reaction of the substituted 2-hydroxybenzaldehydes and phosphonates.[18] The starting aldehydes were prepared from 2-hydroxybenzoic acids **2** (Scheme 1). Esterification of 4-methyl-2-hydroxybenzoic acids (**2a**,**b**) yielded methyl esters and they were protected with a *p*-methoxybenzyl (PMB) group. The esters (**3a**,**b**) were converted to aldehyde (**4a**,**b**) by reduction with lithium aluminum hydride (LAH) and the following oxidation with pyridinium chlorochromate (PCC). The 4-fluorinated aldehyde **4c** was prepared from the alcohol **5** by reacting with paraformaldehyde and the following protection with *p*-methoxybenzyl chloride (PMBCl).

Preparation of phosphonates for Wittig reaction is shown in Scheme 2. The aldehydes (**7**) and 2,2-dimethyl-1,3-dioxane-4,6-dione (meldrum's acid, **8**) was reacted with borane dimethylamine in dry methanol to synthesize the 4,6-dione (**9**). Mannich type reaction of the 4,6-dione (**9**) with *N*,*N*-dimethylmethylene ammonium iodide (Eschenmoser's salt)[19] and the following reaction with triethyl phosphonoacetate and sodium hydride (NaH) gave the phosphonate (**11**).

Wittig reaction with aldehyde (**4a–c**) gave *Z*-isomer **12a–i** (Scheme 3). *p*-Methoxybenzyl (PMB) group was deprotected with hydrochloride and the subsequent cyclization gave the coumarin ring (**14a–i**). The treatment of the ester **14a** with potassium hydroxylamide gave the racemic α-substituted hydroxamate **15a** (Scheme 4). The benzyloxy group on aromatic ring at α-position of coumarin ring (**14b–i**) was deprotected with Pd/C under H_2 atmosphere to give the alcohol **16a–h**. The various alkylated analogues of phenol **16a–h** were prepared by alkylation with 1-(2-chloroethyl)piperidine hydrochloride or *N*,*N*-dialkylaminoethyl chloride to give phenethylether (**17a–l**). The esters were converted to the racemic α-substituted hydroxamate analogues (**15b–l**).

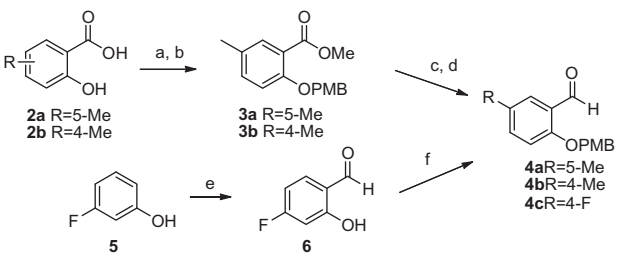

Scheme 1. Reagents and conditions: (a) H_2SO_4, MeOH, reflux; (b) PMBCl, K_2CO_3, KI, acetone, 65 °C; (c) $LiAlH_4$, THF; (d) PCC, SiO_2, CH_2Cl_2; (e) paraformaldehyde, 10% H_2SO_4, MeOH/toluene, reflux; (f) PMBCl, K_2CO_3, DMF.

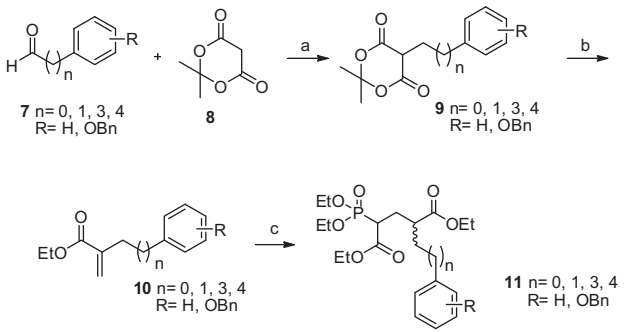

Scheme 2. Reagents and conditions: (a) BH_3Me_2NH, MeOH; (b) Eschenmoser's salt, EtOH, heating; (c) triethyl phosphonoacetate, NaH, THF.

Next, all α-alkoxy aromatic alkyl substituted chromen-based analogues (**15a–l**) designed occupy S1′ pocket of TACE enzyme was evaluated for in vitro and in vivo activities.

2.2. QSAR and docking study

2.2.1. Chemical and biological data

A series of 26 α-substituted chromen-based TACE inhibitors were used for the present study (see Supplementary data, Fig. S1).[18,20] α-Alkoxy aromatic alkyl group substituted chromen-based analogues (**S1a–k**, **S2a–o**) were comprised of 18 molecules in training set and eight molecules in test set. Another set of molecules, γ-lactam hydroxamic acid derivatives (**S3a–d**), represented by DPC-333 (**S3b**)[18,20] were taken from the literature and used only as a test set for the QSAR model.

The biological activities of 26 molecules measured as IC_{50} which ranging from 1 nM to 40 μM against human TACE enzyme. Then, they were converted to pIC_{50} ($pIC_{50} = \log 1/IC_{50}$) so that they can be used in QSAR as dependent variable where IC_{50} is the concentration of the inhibitor producing 50% inhibition of the enzyme. The structure observed and predicted biological activities of the each molecule are presented in Supplementary data (Tables S1–S3). Also all of 26 molecules were prepared and minimized in Discovery Studio 2.5. The energy minimization of each molecule was carried out by the CHARMm force field of Discover program.

2.2.2. Calculation of descriptors and generation of QSAR models

QSAR analysis is an area of computational research which builds models of biological activity using physicochemical properties of a series of compounds. Different types of descriptors were calculated for each molecule in the study table using Discover Studio 2.5 and preADMET. These descriptors include constitutional, electrostatic, geometrical, physicochemical, and topological descriptors (Table S4).

QSAR model generation was performed by genetic function approximation (GFA) technique with Discovery Studio 2.5. The application of GFA algorithm allows the construction of high-quality predictive models and makes additional information not provided by standard regression techniques. GFA was performed using 50,000 crossovers, 1500 population size, and smoothness value of 2.0. The number of terms in the equation was set as initial equation length 4 to maximum equation length 6. The set of equations generated were evaluated with the following notation: r^2 is the coefficient of determination; r^2 (adj) is r^2 adjusted for the number of terms in the model; r^2 (pred) is the prediction (PRESS) r^2, equivalent to q^2 from a leave-1-out cross-validation; Friedman L.O.F. is the Friedman lack-of-fit score; S.O.R. *P*-value is the *P*-value for significance of regression.

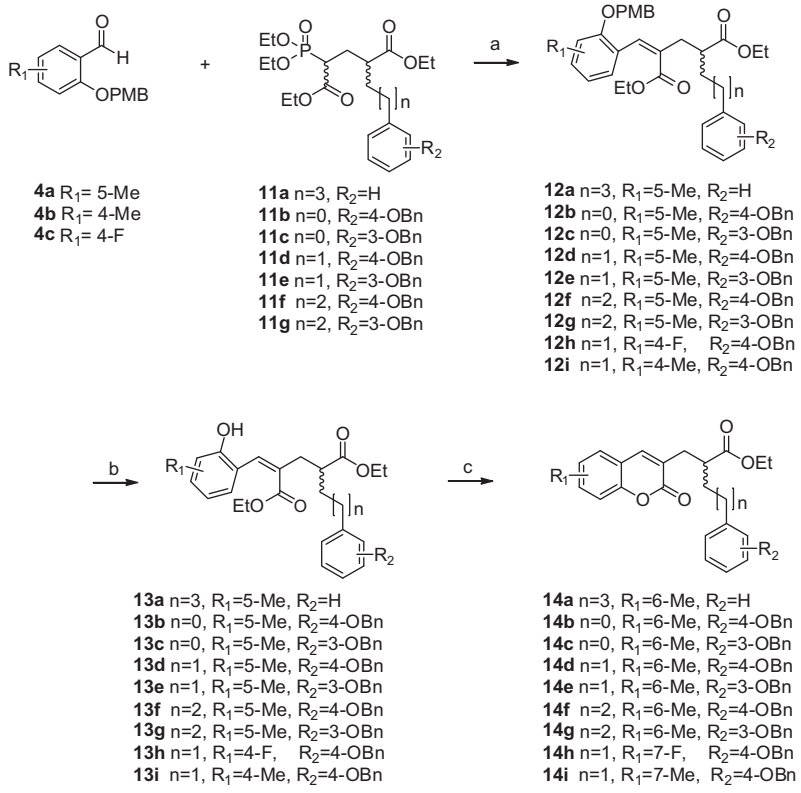

Scheme 3. Reagents and conditions: (a) *t*-BuOLi, THF; (b) 4 N HCl, 1,4-dioxane; (c) xylene, 155 °C.

2.2.3. Docking study

All the molecular docking studies were performed by the docking software LigandFit[21] module of Discovery Studio 2.5 (Accelrys, San Diego, CA). In this paper, the docking of chromen-based TACE inhibitors into the active site of human TACE was performed. The crystal structure of human TACE (pdb code: 3EDZ)[22] obtained from the Protein Data Bank was refined to remove water molecules and to add hydrogen atoms to the whole enzyme under the condition of pH 7.40. A binding pocket of the native ligand (methyl (1*R*,2*S*)-2-(hydroxycarbamoyl)-1-{4-[(2-methylquinolin-4-yl)methoxy]benzyl}cyclopropanecarboxylate) was selected as the binding site for the study. The CFF (Consistent Force Field) function was selected as the energy grid and Monte Carlo trial method was used to roughly search the conformations when compounds are docked into the TACE enzyme. Then the ligands were optimized using a forcefield function, CHARMm. Thirty poses were docked for each ligand. Among the docked conformations, the over-fitted conformation was eliminated and the poses with higher consensus score among LigScore1, LigScore2, PLP1, PLP2, Jain, PMF, and DockScore were selected for further analysis.

3. Results and discussion

3.1. Pharmacological optimization

Series of the racemic α-substituted analogues (**15a–l**) were tested in vitro for inhibition of TACE enzyme and cellular TNF-α and NO production (Table 1). All of the prepared analogues did not inhibit the production of NO on RAW264.7 cells. Most of compounds showed very strong TACE inhibitory activities ranging 0.3–30 nM of IC_{50} values, well correlated with their cellular TNF-α inhibitory activities. The 4-hydroxyphenylethyl analogue (**15b**) showed good activity comparable to the benzyl analogue (**1b**). It has TACE inhibition at 0.3 nM of IC_{50} as well as cellular TNF-α inhibition, but the phenylbutyl analogue (**15a**) showed poor cellular TNF-α inhibitory activity with relatively weak TACE inhibition (IC_{50} = 33 nM). The length between the chromen ring and the aromatic group of **15a** is too long to fit in the S1′ pocket of TACE. Thus, the tertiary aminoethyl groups were introduced to 3- or 4-hydroxyl group on the phenyl rings of the α-benzyl analogues (n = 0), phenethyl analogues (n = 1) and phenpropyl analogues (n = 2) to explore the α-substituent effect. The tertiary amino group on the alkylated group was intended to increase the water solubility. The prepared piperidinylethyl substituted analogues (**15c–h**) showed almost same potencies at around 0.1 nM and 0.2 μM of IC_{50} in inhibition of TACE and cellular TNF-α, respectively, except **15c**. For the benzyl analogues (**15c** and **15d**), 3-position is better than 4-position for in vitro activities. Among these, 4-alkylated phenethyl analogue (**15e**) showed the best IC_{50} as 0.00104 and 0.20 μM for TACE and TNF-α inhibition, respectively. And other close amino analogues of **15e** were prepared. The corresponding dimethylamino analogue (**15i**) and diethylamino analogue (**15j**) were 1.8- and 1.4-fold more potent than **15e** in cellular TNF-α inhibition, respectively. Finally, 7-substituted coumarin analogues (**15k** and **15l**) were prepared to compare in vitro activities to 6-substituent analogues and showed twofold more potent in cellular TNF-α inhibition than **15i**. Among the prepared 12 α-substituted analogues, **15l** showed the most potent in vitro inhibitory activities, 0.28 nM and 60 nM of IC_{50} values for TACE inhibition and the cellular TNF-α inhibition, respectively.

The most potent TACE inhibitor **15l** shows very good selectivity to MMP-1 by 1889 fold but some selectivity to MMP-3 and MMP-9 by only 29-fold and 73-fold, respectively (Table 2). The excellent selectivity of **15l** to MMP-1 gave a good potential to reduce the possible toxicity of TACE inhibition. Though the structural difference of S1′ pocket between TACE and MMPs (MMP-2 and

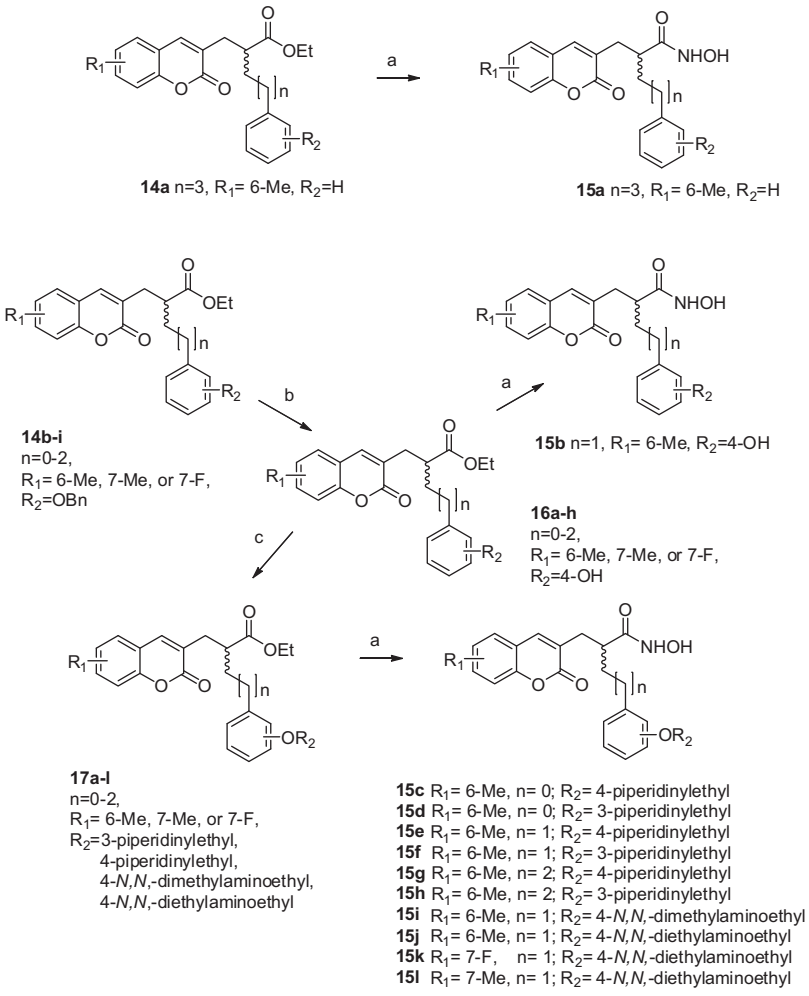

Scheme 4. Reagents and conditions: (a) NH_2OK, MeOH; (i) LiOH, MeOH/THF; (ii) pentafluorophenol, DMAP, EDCI, CH_2Cl_2; (iii) NH_2OK, MeOH; (b) Pd/C, H_2, EtOH; (c) 1-(2-chloroethyl)piperidine hydrochloride, Cs_2CO_3, NaI, DMF, 80–85 °C or 2-chloro-*N*,*N*-dialkylethanamine hydrochloride, NaH, DMF.

MMP-9)[18] is the rationale for design of the selective TACE inhibitor, long α-substituents of chromen-based inhibitors increase the inhibitory activity to TACE as well as MMPs. Thus, **15l** is the dual functional inhibitor to TACE and MMPs.

Compound **15l** showed higher efficacy than DPC-333 in in vivo TNF-α inhibition experiment although it was five times less active than DPC-333 in cellular inhibition of TNF-α in RAW264.7 cells. Orally administered 30 mg/kg of **15l** inhibited 74% of serum TNF-α production in LPS induced endotoxemia animal model whereas DPC-333 showed 61% in the same condition (Table 3). The good in vivo efficacy of **15l** in po administration may be explained by exploring the pharmacokinetic profiles. First, liver microsomal stability, one of several major determining factors for the oral bioavailability and systemic clearance was examined using human liver microsome. As a result, **15l** showed a long half-life ($t_{1/2}$) at 73 min and good microsomal clearance (Table 4). Encouraged by this in vitro result, in vivo pharmacokinetic profiles of **15l** in Sprague–Dawley (SD) rats were evaluated (Table 5). The systemic plasma clearance (CL) was moderate with an average of 2.66 l/h/kg. The apparent volume of distribution at steady state (V_{ss}) was estimated to be 3.04 l/kg indicating that **15l** is likely to be readily distributed inside of the vasculature. The apparent terminal elimination phase in plasma began approximately 5–8 h after dosing, with an average half-life ($t_{1/2}$) of 1.14 h following the intravenous administration. The oral absorption of **15l** in rats was relatively late, with T_{max} occurring at 2.00 h. The apparent terminal elimination phase in plasma appeared to begin at 5 h, with an estimated half-life ($t_{1/2}$) of 3.19 h. The oral bioavailability was 41.6% in rats.

Finally, the pharmacological efficacy of **15l** was evaluated using the acute carrageenan induced arthritis model in SD rat (Fig. 2). The edema reached to maximum 6 h after the induction and the inhibition activity of each test group was determined at 6 h and 12 h after peripheral (ip) injection. The positive control using indomethacin and the two test groups (30 mg/kg and 100 mg/kg of **15l**) inhibited rat paw edema by 15%, 8%, and 20% at 6 h, and 4%, 14%, and 35% at 24 h, respectively, compared to the vehicle. Accordingly, it was proved that **15l** effectively inhibited rat paw edema.

3.2. Docking and QSAR study

3.2.1. GFA models

In the present study, QSAR model was generated using the training set of α-alkoxyaryl alkyl group substituted chromen-based analogues. Test set with regularly distributed biological activities was used to evaluate the predictive ability of the generated QSAR models.

Six descriptors namely *Balaban_index_JX*, *FNSA3*, *Log D*, *Num_Atoms*, *Num_Chains*, and *WNSA2*, significantly explain the variance in the biological activity for α-alkoxyaryl alkyl substituted

Table 1
In vitro inhibitory activities of compounds **15a–l**

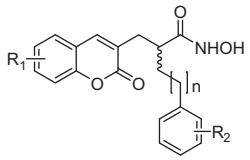

Compound	R_1	*n*	R_2	IC_{50}[a] (μM)		
				TACE	TNF-α[b]	NO[b]
DPC-333	—	—	—	0.00010	0.012	NA
1b	6-Me	0	H	0.00050	0.52	NA
15a	6-Me	3	H	0.03282	>3.0	NA
15b	6-Me	1	OH	0.00030	0.92	NA
15c	6-Me	0	4-(2-Piperidin-1-yl-ethoxy)	0.01094	1.5	NA
15d	6-Me	0	3-(2-Piperidin-1-yl-ethoxy)	0.00107	0.26	NA
15e	6-Me	1	4-(2-Piperidin-1-yl-ethoxy)	0.00104	0.20	NA
15f	6-Me	1	3-(2-Piperidin-1-yl-ethoxy)	0.00090	0.24	NA
15g	6-Me	2	4-(2-Piperidin-1-yl-ethoxy)	0.00107	0.32	NA
15h	6-Me	2	3-(2-Piperidin-1-yl-ethoxy)	0.00027	0.23	NA
15i	6-Me	1	4-(2-Dimethylamino-ethoxy)	0.00066	0.11	NA
15j	6-Me	1	4-(2-Diethylamino-ethoxy)	0.00053	0.14	NA
15k	7-F	1	4-(2-Dimethylamino-ethoxy)	0.00046	0.07	NA
15l	7-Me	1	4-(2-Dimethylamino-ethoxy)	0.00028	0.06	NA

[a] Values are means of three experiments.
[b] RAW264.7 cells were used, NA = no inhibition at 10 μM.

Table 2
In vitro inhibitory activities of compound **15l** and DPC-333

Compound	IC_{50}[a] (μM)			
	TACE	MMP-1	MMP-3	MMP-9
15l	0.00031	557	8.7	23
DPC-333	0.00010	4926	3.9	460

[a] Values are means of three experiments.

Table 3
In vivo inhibition of LPS induced TNF-α by **15l** and DPC-333

Compound	Dose (mg/kg)	% Inhibition[a]
15l	30 (po)	74%**
DPC-333	30 (po)	61%**

LPS (1.5 mg/kg, ip) was pre-treated twice (ip) at 24 h and 0.5 h before **15l** and DPC-333 were orally administered. Serum TNF-α was measured after 60 min. *P <0.05; **P <0.01.
[a] BALB/c mice (four per group) were treated.

Table 4
Human liver microsomal stability of **15l**

Compound	$t_{1/2}$ (min)	Microsomal clearance (μL/mim/mg)
15l	73.0	9.5
DPC-333	94.5	7.3

15l and DPC-333 (40 μM) was incubated with human liver microsomes (1 mg/mL) in the presence of NADPH (1 mM), followed by liquid chromatography MS/MS mass spectrometry analysis. The analytical data were processed by Metabolite ID™ program.

Table 5
In vivo pharmacokinetic profiles of **15l**

Parameter	Unit	iv (N = 3)	po (N = 3)
Dose	(mg/kg)	5.00	30.00
T_{max}	(h)	—	2.00
C_{max}	(μg/ml)	—	1.14
AUC_{0-inf}	(h μg/ml)	1.88	4.69
CL	(l/h/kg)	2.66	—
V_{ss}	(l/kg)	3.04	—
$t_{1/2}$	(h)	2.80	3.19
MRT_{inf}	(h)	1.14	2.90
F	(%)	—	41.61

Sprague–Dawley (SD) rats were used.

chromen-based analogues in equation (1) (Table 6). The variance of this model was found to be 88%. The equation (1) also shows good correlation coefficient for leave-one-out validation (r^2 (pred)) with 80% of the variance. The correlation coefficient (r^2) between observed and predicted activity of test set was found to be 0.7719 (Fig. 3). The constitutional descriptors, *Num_Atoms* and *Num_Chains*, positively correlate with biological activity. It underlines the importance of size of molecules. *FNSA3* and *WNSA2* which are electrostatic descriptors, denote the fractional negative surface area computed with quantum charges and weighted negatively charged partial surface area, respectively. Though these descriptors have similar components, the equation (1) is weighted more on *FNSA3* rather than *WNSA2* as shown on coefficients. *Balaban_index_JX* is a topological descriptor weighted on relative electronegativity, and Log *D* is the octanol–water partition coefficient calculated by taking the ionization states of the molecule which represents lipophilicity of a molecule into account.

3.2.2. Docking study and binding mode analysis

To understand the interactions between the TACE and its inhibitors and to explore their binding mode, docking study was performed using LigandFit[21] of Discovery Studio 2.5. The active site cleft of TACE is deep and contains zinc, and the right-hand side of the zinc corresponds to the S1′, S2′, and S3′ pocket. The ligand–enzyme interaction analysis shows that Thr347, Leu348, Gly349, His405, Glu406, and His409 are the important residues at the

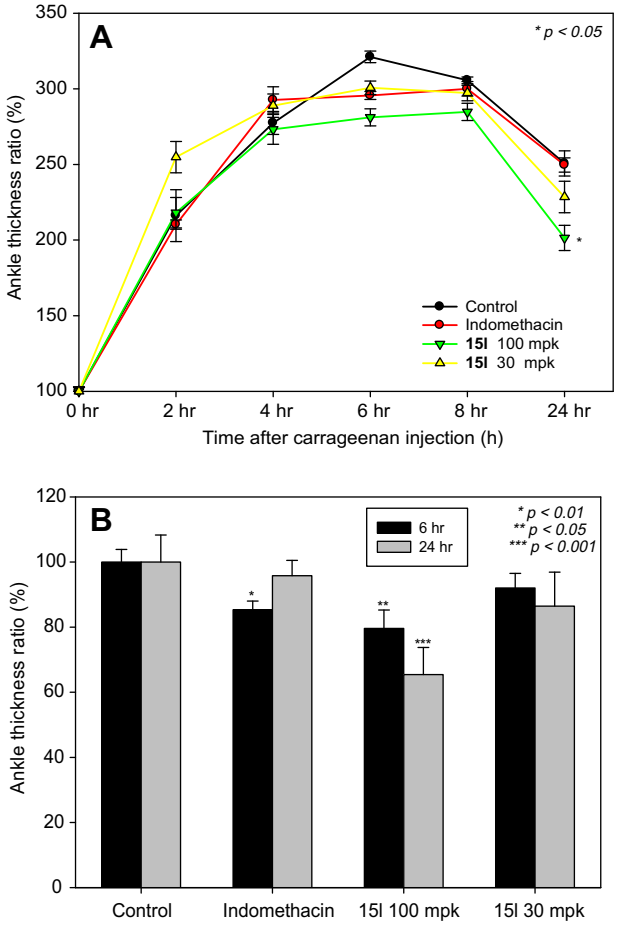

Figure 2. (A) Effects of **15l** on carrageenin induced paw edema model in SD rat. (B) Effects of inhibition of indomethacin, **15l** (30 mg/kg) and **15l** (100 mg/kg) on paw edema at 6 h and 24 h after carrageenan induction. The edema reached maximum 6 h after the induction and the inhibition activity compared to vehicle was determined at 6 h and 12 h after peripheral (ip) injection. Indomethacin (10 mg/kg) was used for the positive control. ($^{*}P$ <0.05; $^{**}P$ <0.01).

active site and are the main contributors to the receptor–ligand interaction.

For α-alkoxyaryl alkyl group substituted chromen-based analogues which are bulky and long, the α-substituent comes into the deep S1′ pocket merged with S3′ pocket. The chromen ring extends away from the enzyme, but still the carbonyl group in chromen ring forms hydrogen bond with the amide nitrogen proton of Leu348 and/or hydroxyl group of Thr347. It also has pi–pi interaction between imidazole ring of His405 of TACE and α-aromatic ring of ligand. Another hydrogen bond has been formed between oxygen on α-alkoxyaromatic ring and amine nitrogen proton on imidazole ring of His405. Thus α-alkoxy aromatic alkyl group substituents fit well in the pocket of the enzyme through S1′ to S3′. (Fig. 4) While S1′ pocket has hydrophobic surface inside, partial positive surface was observed in adjacent to S3′ pocket. *FNSA3* stands for the sum of each surface area for a negatively charged atom multiplied by negative charge divided by the total surface area. Because it is multiplied by a negative charge, *FNSA3* has negative value. Thus surface area for a negatively charged atom should be increased for better activity. The receptor–ligand interaction is stabilized by van der Waals interaction between alkoxy moiety of α-alkoxy aromatic alkyl group substituent and positive charged S3′. This is also proved by negative correlation of Log *D*, signifying lipophilicity of a molecule, to the biological activity. The docking study of **15l**, which showed the best in vitro and in vivo pharmacokinetic profiles among 12 synthesized analogues, also fitted well into the QSAR equation. (Fig. 5) Moreover, the (*S*)-isomer of **15l** was docked into the catalytic domains of the human TACE and MMP-3 (1G49.pdb)[23] enzyme. The docking data suggest that the hydroxamic acid moiety of **15l** binds the zinc metal in the active sites of TACE and MMP-3 enzyme. The carbonyl group in chromen ring interacts with the hydroxyl group of Thr347 of TACE through hydrogen bonding whereas the carbonyl group of chromen ring forms a hydrogen bonding with the Leu664 of MMP-3. This difference on the docking poses between TACE and MMP-3 explains the TACE selectivity of **15l** over MMP-3. It should also be pointed out that the only (*S*)-configuration of α-position of hydroxamic acid would be allowed to fit into the empty S1′ pocket of TACE and could afford an extra stabilization through the hydrogen bonding between the oxygen at the α-position of hydroxamic acid and the hydrogen of imidazole ring of His405, and the pi–pi interaction between α-aromatic ring of **15l** and imidazole ring of His405 of TACE.

Finally, the docking study suggests that the α-alkoxy aromatic alkyl group substituted chromen-based analogues are stabilized by binding inside the active cleft (S1′ and S3′) of TACE, due to the presence of an extra hydrogen bond and van der Waals interaction. Thus, the QSAR equation may be useful for the design and development of novel α-substituted chrome-based TACE inhibitor having better inhibitory activity.

3.2.3. Validation

For the external validation, four γ-lactam hydroxamate derivatives[18,20] were used as an additional test set. It has been previously shown that van der Waals interaction between the fractional negative surface area of α-alkoxyaryl alkyl substituent and the amino acid residues inside the S1′ pocket increases biological activity of TACE. Thus, four γ-lactam hydroxamate derivatives were selected because of the similarity in α-alkoxy aromatic ring. (Table S3) The test set was applied in equation (1) and the squared regression coefficient (r^2) resulted as 0.8849. (Fig. 3) The model is illustrated on a specific case, comparing **S3d** with **S3a** and **S3c**. Compound **S3d** has benzyloxy group for alkoxy aromatic moiety of α-position when **S3a** and **S3c** has electron density rich atom. The negative correlation of *FNSA3* and Log *D* could be elucidated and demonstrated by this example. Another set of compound, **S3b** and **S3c**, could also validate the equation with size-related descriptors, *Num_Atoms* and *Num_Chains*. Compound **S3b**, which has bulky group (*iso*-butyl) that may place on S1 pocket of TACE, showed better inhibitory activity than compound **S3c** which has simple methyl group (Table S3).

Table 6
QSAR equations generated using genetic function approximation for the training set of the molecules in each group

No.	Equation	r^2	r^2 (adj)	r^2 (pred)	RMS residual error	Friedman L.O.F.	S.O.R. *P*-value
1	pIC_{50} = −120.91 + 12.369 (Balaban_index_JX) − 736.95 (FNSA3) − 0.85767 (Log *D*) + 1.5867 (Num_Atoms) + 1.0541 (Num_Chains) + 0.070294 (WNSA2)	0.9214	0.8785	0.7978	0.2687	0.1045	1.79 E^{-05}

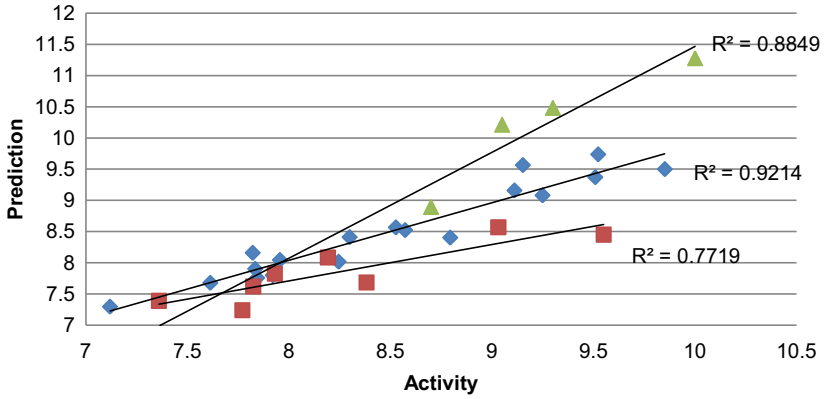

Figure 3. A graph of actual versus predicted activities of training set (♦) and test sets (■ and ▲ (**S3**)) of molecules using equation (1). Balaban_index_JX: relative electronegativity; FNSA3: fractional charged partial negative surface area third type; Log *D*: the octanol–water partition coefficient calculated taking into account the ionization states of the molecule; Num_Atoms: heavy atoms; Num_Chains: unbranched chains needed to cover all the non-ring bonds in the molecule; WNSA2: surface weighted charged partial negative surface area second type.

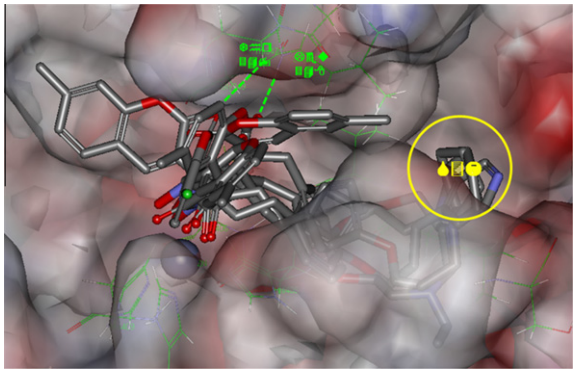

Figure 4. Docked conformations of α-alkoxyaryl alkyl group substituted chromen-based analogues (**S1a**, **S1i**, **S2k**, **S2m**, and **S2n**): The α-substituents of TACE inhibitors binds through the S1′ to S3′ pocket, which is the active site of TACE enzyme. And the hydrogen bond between the carboxyl group of the chromen ring and Thr347 or Leu348 of TACE enzyme fixes the chromen ring on the surface of S1 pocket. Depending on the α-substituents, the chromen ring could be rotated and placed on different directions on the surface of S1 pocket.

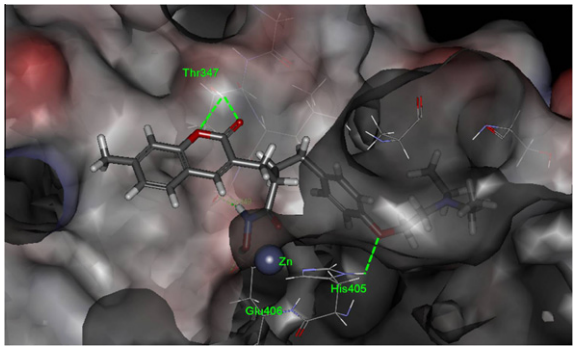

Figure 5. The docking model for the (*S*)-α-substituted chromen analogue (**15l**) binding to the binding pocket of TACE.

According to the result, pyrrolidinone in γ-lactam hydroxamates would replace alkyl group in α-alkoxy aromatic alkyl substituted chromen-based analogues. The binding modes of γ-lactam hydroxamates also support the result. (Fig. 6) The carbonyl group on pyrrolidinone ring also plays a role as a hydrogen bond acceptor like the carbonyl group on chromen ring. And the alkoxy aromatic

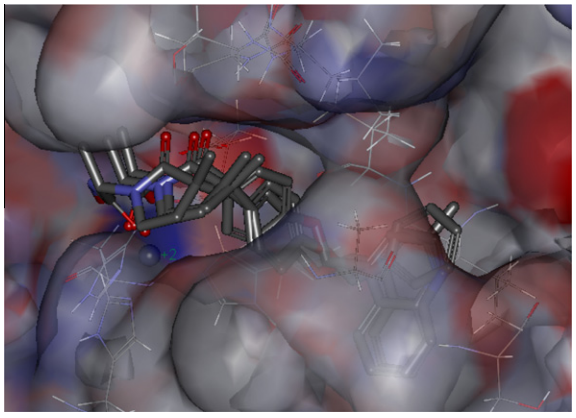

Figure 6. Docked conformations of γ-lactam hydroxamic acid derivatives (**S3a**, **S3c**, and **S3d**).

moiety at α-position of γ-lactam hydroxamates give extra stabilization for the receptor–ligand interaction.

4. Conclusion

A series of α-substituted chromen-core TACE inhibitors were rationally designed for filling in S1′ pocket of the enzyme. Twelve analogues were synthesized by varying the chain length and alkylation pattern on aromatic ring of side chain. Most of compounds were active in vitro TACE enzyme inhibition as well as cellular TNF-α inhibition. Among these, **15l** showed most promising in vitro and in vivo activity profiles. Based on these results, **15l** was evaluated on in vitro and in vivo pharmacokinetic studies and found moderate systemic clearance and good oral bioavailability at 42%. It was also evaluated in carrageenan induced RA animal model and found that it effectively inhibited paw edema in rat. QSAR study and docking were also performed to confirm the series of α-alkoxyaryl alkyl substituted chromen-based analogues. α-Substituent with long and bulky groups of coumarin core TACE inhibitors, gets inside the S1′ and S3′ pocket and formed van der Waals interaction so that increases the inhibitory activity. Hence, the docking studies suggest that α-alkoxyaryl alkyl group shows great activity by stabilizing receptor–ligand interaction. Also the docking study of **15l** showed the dual function inhibitory activity to TACE and MMP-3. On the basis of the descriptors thus obtained from the QSAR equation, novel α-substituted chromen-based TACE

inhibitors can be designed and developed that are predicted to attain improved TACE inhibitory activity.

5. Experimental

All chemicals were obtained from commercial suppliers and used without further purification. Flash column chromatography was performed with silica (Merck EM9385, 230–400 mesh). ^{1}H and ^{13}C NMR spectra were recorded at 300 and at 75 MHz, respectively. Proton and carbon chemical shifts are expressed in ppm relative to internal tetramethylsilane, and coupling constants (*J*) are expressed in Hertz. LC/MS (liquid chromatography–mass spectrometry) spectra were recorded by electrospray ionization (ESI) on Shimazu LC/MS instruments (20% 0.1% TFA in H_2O/0.1% TFA in acetonitrile) scan (from 0 to 600 amu/z) mode and the detected ion peaks are $(M+z)/z$ and $(M-z)/z$ in positive and negative ion mode, respectively, where *M* represents the molecular weight of the compound and *z* the charge (number of protons). LC/MS/MS were recorded by electrospray ionization (ESI) on Agilent 1100/API2000 system. HRMS (High resolution mass spectrometry) were obtained from fast atom bombardment (FAB) on JMS-700 (Jeol, Japan) High Resolution Tandem Mass Spectrometry in Korea Basic Science Institute in Seoul, Korea. Final products were purified to a minimum purity of 96%, as determined by reversed phase HPLC (see Supplementary data: Table S5).

5.1. Procedures for 4a–c

5.1.1. Methyl 2-(4-methoxybenzyloxy)-5-methylbenzoate (3a)

2-Hydroxy-5-methylbenzoic acid (**2a**, 12.0 g, 78.9 mmol, 1.0 equiv) was dissolved in MeOH (100 mL) and H_2SO_4 (1.2 mL) was added at room temperature. The mixture was heated at reflux for 2 days (TLC). The mixture was cooled to room temperature. $NaHCO_3$ Solution was added to reaction mixture and then the mixture was extracted with ethyl acetate. The organic layer was washed with brine, dried over anhydrous $MgSO_4$, filtered, and concentrated. The residue was purified by column chromatography on silica gel (hexane/ethyl acetate = 3:1) to give the ester (12.0 g, 91%); ^{1}H NMR ($CDCl_3$, 400 MHz) δ 10.57 (s, 1H), 7.61 (d, *J* = 2.0 Hz, 1H), 7.25 (d, *J* = 8.4 Hz, 2.0, 1H), 6.87 (d, *J* = 8.4 Hz, 1H), 3.92 (s, 3H), 2.27 (s, 3H).

4-Methoxybenzyl chloride (10.7 mL, 78.8 mmol, 1.1 equiv) was added to a solution of the above ester (11.9 g, 71.6 mmol, 1.0 equiv), K_2CO_3 (29.7 g, 214.8 mmol, 3.0 equiv) and KI (1.2 g, 7.16 mmol, 0.1 equiv) in acetone (100 mL) at room temperature. The mixture was heated at 65 °C for 12 h (TLC). The mixture was cooled at room temperature. Water was added to the reaction mixture and then the mixture was extracted with ethyl acetate. The organic layer was washed with brine, dried over anhydrous $MgSO_4$, filtered, and concentrated. The residue was purified by column chromatography on silica gel (hexane/ethyl acetate = 4:1) to give compound **3a** (19.0 g, 93%); ^{1}H NMR ($CDCl_3$, 400 MHz) δ 7.62 (d, *J* = 2.0 Hz, 1H), 7.41 (d, *J* = 8.8 Hz, 2H), 7.22 (d, *J* = 8.4 Hz, 2.0, 1H), 6.92–6.90 (m, 3H), 5.08 (s, 2H), 3.89 (s, 3H), 3.81 (s, 3H), 2.30 (s, 3H); MS (ESI) *m/z* 309 (MNa^+).

5.1.2. 2-(4-Methoxybenzyloxy)-5-methylbenzaldehyde (4a)

LAH (2.52 g, 66.4 mmol, 1.0 equiv) was added to a solution of **3a** (19.0 g, 66.4 mmol, 1.0 equiv) in THF (200 mL) at 0 °C. The reaction mixture was warmed to room temperature and then stirred for 30 min. H_2O (2.5 mL), 15% NaOH aqueous solution (2.5 mL) and H_2O (2.5 mL) were added sequently to the reaction mixture. The white solid was filtered through pad of Celite and the solvent was evaporated to give the alcohol (17.1 g, 99%); ^{1}H NMR ($CDCl_3$, 400 MHz) δ 7.44 (d, *J* = 8.4 Hz, 2H), 7.11 (d, *J* = 2.0 Hz, 1H), 7.06 (d, *J* = 8.4 Hz, 2.0, 1H), 6.92 (d, *J* = 8.4 Hz, 2H), 6.86 (d, *J* = 8.4 Hz, 1H), 5.02 (s, 2H), 4.67 (s, 2H), 3.82 (s, 3H), 2.46 (br, 1H), 2.30 (s, 3H).

PCC (42.5 g, 197.4 mmol, 3.0 equiv) and SiO_2 (42.5 g) were added to a solution of the above alcohol (17.0 g, 65.8 mmol, 1.0 equiv) in methylene chloride (200 mL). The mixture was stirred at room temperature for 1 h. The reaction mixture was filtered through pad of Celite. The filtrate was concentrated and purified by column chromatography on silica gel (hexane/ethyl acetate = 3:1) to give compound **4a** (16.4 g, 97%); ^{1}H NMR ($CDCl_3$, 400 MHz) δ 10.49 (s, 1H), 7.64 (d, *J* = 2.0 Hz, 1H), 7.36–7.34 (m, 3H), 6.96 (d, *J* = 8.8 Hz, 2H), 6.92 (d, *J* = 8.8 Hz, 1H), 5.09 (s, 2H), 3.82 (s, 3H), 2.31 (s, 3H); MS (ESI) *m/z* 279 (MNa^+).

5.1.3. 2-(4-Methoxybenzyloxy)-4-methylbenzaldehyde (4b)

^{1}H NMR ($CDCl_3$, 400 MHz) δ 10.45 (s, 1H), 7.75 (d, *J* = 8.0 Hz, 1H), 7.37 (d, *J* = 8.4 Hz, 2H), 6.94 (d, *J* = 8.4 Hz, 2H), 6.87 (s, 1H), 6.85 (d, *J* = 8.0 Hz, 1H), 5.10 (s, 2H), 3.83 (s, 3H), 2.40 (s, 3H); MS (ESI) *m/z* 279 (MNa^+).

5.1.4. 4-Fluoro-2-hydroxybenzaldehyde (6)

3-Fluorophenol (**5**, 5.0 ml, 56.0 mmol, 1.0 equiv) was added to 8 wt % magnesium methoxide solution in MeOH (44.5 mL) and the mixture was distilled. Approximately, half of the methanol was distilled off and toluene (42 mL) was added and the azeotropic mixture was removed by fractional distillation until the temperature of the reaction mixture rose to 95 °C. Slurry of paraformaldehyde powder (5.18 g, 172.5 mmol, 3.1 equiv) in toluene (10 mL) was added in small portion over 1 h with concurrent removal of volatile materials by distillation. The mixture was stirred at 95 °C for 1 h and cooled to room temperature. The reaction mixture was added slowly to 10% sulfuric acid solution (63 mL) and stirred at 30–40 °C for 2 h. The reaction mixture was extracted with toluene, washed with 10% sulfuric acid solution and water, dried over anhydrous $MgSO_4$, filtered, and concentrated in vacuo. The residue was purified by column chromatography on silica gel (hexane/ethyl acetate = 8:1) to give compound **6** (4.05 g, 52%); ^{1}H NMR ($CDCl_3$, 400 MHz) δ 11.37 (s, 1H), 9.84 (s, 1H), 7.57 (dd, *J* = 8.6, 6.4 Hz, 1H), 6.76–6.66 (m, 2H).

5.1.5. 4-Fluoro-2-(4-methoxybenzyloxy)benzaldehyde (4c)

4-Methoxybenzyl chloride (0.85 mL, 6.6 mmol, 1.1 equiv) was added to a solution of **59** (0.85 g, 6.0 mmol, 1.0 equiv), K_2CO_3 (2.50 g, 18.1 mmol, 3.0 equiv) in DMF (6 mL) at room temperature. The mixture was stirred at room temperature for 12 h. Water was added to the reaction mixture and then the mixture was extracted with ethyl acetate. The organic layer was washed with brine, dried over anhydrous $MgSO_4$, filtered, and concentrated. The residue was purified by column chromatography on silica gel (hexane/ethyl acetate = 6:1) to give compound **4c** (1.45 g, 92%); ^{1}H NMR ($CDCl_3$, 400 MHz) δ 10.40 (s, 1H), 7.87 (dd, *J* = 8.6, 6.4 Hz, 1H), 7.36 (d, *J* = 8.4 Hz, 2H), 6.94 (d, *J* = 8.4 Hz, 2H), 6.78–6.71 (m, 2H), 5.09 (s, 2H), 3.83 (s, 3H); MS (ESI) *m/z* 261 (MH^+).

5.2. General procedures for 9

Meldrum's acid (**8**, 1.0 equiv) was added to a solution of borane dimethylamine complex (1.0 equiv) in MeOH (0.5–1 M solution). Benzaldehyde **7** (3.0 equiv) in MeOH (1 M solution) was added dropwise to the mixture and then stirred at room temperature for 20 min and the reaction mixture was stirred at room temperature for 30 min. Ice water was added to the reaction mixture and the solution was acidified with 2 N HCl to pH 1. The mixture was stirred at 0 °C for 1 h and the solid was filtered and washed with water to give compound **9** in 60–80% yield.

5.2.1. 2,2-Dimethyl-5-(4-phenylbutyl)-1,3-dioxane-4,6-dione

^{1}H NMR ($CDCl_3$, 400 MHz) δ 7.29–7.16 (m, 5H), 3.49 (t, J = 5.2 Hz, 1H), 2.63 (t, J = 7.6 Hz, 2H), 2.16–2.11 (m, 2H), 1.77 (s, 3H), 1.75 (s, 3H), 1.72–1.49 (m, 4H); MS (ESI) m/z 277 (MH^+).

5.2.2. 5-(4-(Benzyloxy)benzyl)-2,2-dimethyl-1,3-dioxane-4,6-dione

^{1}H NMR ($CDCl_3$, 400 MHz) δ 7.43–7.32 (m, 5H), 7.23 (d, J = 8.8 Hz, 2H), 6.89 (d, J = 8.8 Hz, 2H), 5.04 (s, 2H), 3.72 (t, J = 4.8 Hz, 1H), 3.44 (d, J = 4.8 Hz, 2H), 1.72 (s, 3H), 1.46 (s, 3H); MS (ESI) m/z 341 (MH^+).

5.2.3. 5-(3-(Benzyloxy)benzyl)-2,2-dimethyl-1,3-dioxane-4,6-dione

^{1}H NMR ($CDCl_3$, 400 MHz) δ 7.44–7.18 (m, 6H), 6.97–6.84 (m, 3H), 5.05 (s, 2H), 3.74 (t, J = 4.8 Hz, 1H), 3.46 (d, J = 4.8 Hz, 2H), 1.73 (s, 3H), 1.50 (s, 3H); MS (ESI) m/z 341 (MH^+).

5.2.4. 5-(3-(Benzyloxy)phenethyl)-2,2-dimethyl-1,3-dioxane-4,6-dione

^{1}H NMR ($CDCl_3$, 400 MHz) δ 7.45–7.20 (m, 6H), 6.88–6.83 (m, 3H), 5.05 (s, 2H), 3.48 (t, J = 5.2 Hz, 1H), 2.84 (t, J = 7.5 Hz, 2H), 2.43–2.38 (m, 2H), 1.76 (s, 3H), 1.73 (s, 3H).

5.3. General procedures for 10

A mixture of **9** (1.0 equiv) and *N*,*N*-dimethylmethyleneiminium iodide (2.5 equiv) in EtOH (0.5 M solution) was stirred at 85 °C. After 4.5 h, reaction mixture was concentrated and extracted with ethyl acetate. The organic layer was washed with $NaHCO_3$ solution, dried over anhydrous $MgSO_4$, filtered, and concentrated to give compound **10** in 70–90% yield.

5.3.1. Ethyl 2-methylene-6-phenylhexanoate

^{1}H NMR ($CDCl_3$, 400 MHz) δ 7.29–7.16 (m, 5H), 6.12 (d, J = 1.2 Hz, 1H), 5.49 (d, J = 1.2 Hz, 1H), 4.20 (q, J = 7.2 Hz, 2H), 2.63 (t, J = 7.6 Hz. 2H), 2.33 (t, J = 7.6 Hz, 2H), 1.67–1.50 (m, 4H), 1.29 (t, J = 7.2 Hz, 3H); MS (ESI) m/z 233 (MH^+).

5.3.2. Ethyl 2-(4-(benzyloxy)benzyl)acrylate

^{1}H NMR ($CDCl_3$, 400 MHz) δ 7.44–7.32 (m, 5H), 7.18 (d, J = 8.8 Hz, 2H), 6.91 (d, J = 8.8 Hz, 2H), 6.20 (d, J = 1.4 Hz, 1H), 5.44 (d, J = 1.4 Hz, 1H), 5.04 (s, 2H), 4.18 (q, J = 7.2 Hz, 2H), 3.57 (s, 2H), 1.27 (t, J = 7.2 Hz, 3H); MS (ESI) m/z 297 (MH^+).

5.4. General procedures for 11

NaH (2.5 equiv) was added to a solution of triethyl phosphonoacetate (1.0 equiv) in THF (0.5 M solution) at 0 °C. After 30 min, **10** (1.0 equiv) in THF (1 M solution) was added and the reaction mixture was stirred at room temperature for 12 h. The mixture was poured into ice water and extracted with ethyl acetate. The organic layer was washed with brine, dried over anhydrous $MgSO_4$, filtered, and concentrated. The residue was purified by column chromatography on silica gel (hexane/ethyl acetate = 1:1) to give compound **11** in 40–50% yield.

5.4.1. Diethyl 2-(4-(benzyloxy)benzyl)-4-(diethoxyphosphoryl)-pentanedioate

^{1}H NMR ($CDCl_3$, 400 MHz) δ 7.43–7.32 (m, 5H), 7.06 (d, J = 8.0 Hz, 2H), 6.87 (d, J = 8.0 Hz, 2H), 5.03 (s, 2H), 4.21–4.02 (m, 8H), 3.10–2.05 (m, 6H), 1.35–1.24 (m, 12H); MS (ESI) m/z 543 (MNa^+).

5.4.2. Diethyl 2-(diethoxyphosphoryl)-4-(4-phenylbutyl)-pentanedioate

^{1}H NMR ($CDCl_3$, 400 MHz) δ 7.29–7.15 (m, 5H), 4.21–4.06 (m, 8H), 3.02–2.92 (m, 1H), 2.61–2.03 (m, 5H), 1.73–1.47 (m, 6H), 1.39–1.20 (m, 12H); MS (ESI) m/z 479 (MNa^+).

5.5. General procedures for 12

One molar *t*-BuOLi (1.5 equiv, THF solution) was added to a solution of **11** (1.5 equiv) in THF (0.2 M solution) and the mixture was stirred at room temperature for 30 min. Compound **4** (1.0 equiv) was added and then the reaction mixture was stirred at room temperature for 12 h. The reaction mixture was extracted with ethyl acetate. The organic layer was washed with brine, dried over anhydrous $MgSO_4$, filtered, and concentrated. The residue was purified by column chromatography on silica gel (hexane/ethyl acetate = 3:1) to give **12** in 80–90% yield.

5.5.1. Diethyl 2-(2-(4-methoxybenzyloxy)-5-methylbenzylidene)-4-(4-phenylbutyl)pentane-dioate (12a)

^{1}H NMR ($CDCl_3$, 400 MHz) δ 7.87 (s, 1H), 7.31 (d, J = 8.4 Hz, 2H), 7.26–7.10 (m, 6H), 7.06 (d, J = 8.4 Hz, 1H), 6.89 (d, J = 8.4 Hz, 2H), 6.83 (d, J = 8.4 Hz, 1H), 4.98 (s, 2H), 4.25 (q, J = 7.2 Hz, 2H), 4.06–3.94 (m, 2H), 3.80 (s, 3H), 2.86–2.64 (m, 3H), 2.51 (t, J = 7.6 Hz, 2H), 2.29 (s, 3H), 1.57–1.41 (m, 4H), 1.33 (t, J = 7.2 Hz, 3H), 1.27–1.16 (m, 2H), 1.12 (t, J = 7.2 Hz, 3H); MS (ESI) m/z 581 (MNa^+).

5.5.2. Diethyl 2-(4-(benzyloxy)benzyl)-4-(2-(4-methoxybenzyloxy)-5-methylbenzylidene)-pentanedioate (12b)

^{1}H NMR ($CDCl_3$, 400 MHz) δ 7.89 (s, 1H), 7.42–7.39 (m, 8H), 7.08–6.97 (m, 4H), 6.87–6.79 (m, 4H), 5.00 (s, 2H), 4.98 (s, 2H), 4.26–4.21 (m, 2H), 3.94–3.85 (m, 2H), 3.79 (s, 3H), 2.97–2.63 (m, 5H), 2.29 (s, 3H), 1.34–1.25 (m, 3H), 1.03–0.99 (m, 3H).

5.5.3. Diethyl 2-(4-(benzyloxy)phenethyl)-4-(2-(4-methoxybenzyloxy)-4-methylbenzyl-idene)pentanedioate (12i)

^{1}H NMR ($CDCl_3$, 400 MHz) δ 7.89 (s, 1H), 7.43–7.30 (m, 7H), 7.18 (d, J = 7.6 Hz, 1H), 6.99 (d, J = 8.8 Hz, 2H), 6.89 (d, J = 8.8 Hz, 2H), 6.83 (d, J = 8.8 Hz, 2H), 6.78 (d, J = 7.6 Hz, 1H), 6.74 (s, 1H), 5.01 (s, 2H), 4.96 (s, 2H), 4.23–3.98 (m, 4H), 3.80 (s, 3H), 2.87–2.69 (m, 3H), 2.44–2.39 (m, 2H), 2.34 (s, 3H), 1.90–1.60 (m, 2H), 1.31–1.18 (m, 6H); MS (ESI) m/z 659 (MNa^+).

5.6. General procedures for 13

4 N HCl (1 equiv, in 1,4-dioxane solution) was added to a solution of **12** in 1,4-dioxane (0.1 M solution) and the mixture was stirred at room temperature for 3 h. The reaction mixture was extracted with ethyl acetate. The organic layer was washed with brine, dried over anhydrous $MgSO_4$, filtered, and concentrated. The residue was purified by column chromatography on silica gel (hexane/ethyl acetate = 3:1) to give compound **13** in 70–80% yield.

5.6.1. Diethyl 2-(2-hydroxy-5-methylbenzylidene)-4-(4-phenylbutyl)pentanedioate (13a)

^{1}H NMR ($CDCl_3$, 400 MHz) δ 7.66 (s, 1H), 7.27–7.00 (m, 6H), 6.92 (s, 1H), 6.78 (d, J = 8.4 Hz, 1H), 5.66 (s, 1H), 4.29–3.92 (m, 4H), 2.73–2.59 (m, 3H), 2.53 (t, J = 7.6 Hz, 2H), 2.27 (s, 3H), 1.61–1.20 (m, 6H), 1.34 (t, J = 7.2 Hz, 3H), 1.13 (t, J = 7.2 Hz, 3H); MS (ESI) m/z 461 (MNa^+).

5.6.2. Diethyl 2-(4-(benzyloxy)benzyl)-4-(2-hydroxy-5-methylbenzylidene)pentanedioate (13b)

^{1}H NMR ($CDCl_3$, 400 MHz) δ 7.69 (s, 1H), 7.43–7.30 (m, 5H), 7.03–6.77 (m, 7H), 5.79 (br, 1H), 5.01 (s, 2H), 4.27–4.22 (m, 2H),

4.01–3.84 (m, 2H), 2.99–2.60 (m, 5H), 2.27 (s, 3H), 1.32 (t, J = 7.2 Hz, 3H), 1.26 (t, J = 7.2 Hz, 3H).

5.6.3. Diethyl 2-(4-(benzyloxy)phenethyl)-4-(2-hydroxy-4-methylbenzylidene)pentane-dioate (13i)

^{1}H NMR ($CDCl_3$, 400 MHz) δ 7.69 (s, 1H), 7.44–7.29 (m, 6H), 7.03–6.98 (m, 2H), 6.89–6.85 (m, 2H), 6.73 (d, J = 8.0 Hz, 1H), 6.69 (s, 1H), 5.65 (br, 1H), 5.03 (s, 2H), 4.26–3.93 (m, 4H), 2.82–2.42 (m, 5H), 2.30 (s, 3H), 1.92–1.65 (m, 2H), 1.30 (t, 7.0 Hz, 3H), 1.17 (t, J = 7.0 Hz, 3H); MS (ESI) m/z 539 (MNa^+).

5.7. General procedures for 14

A solution of **14** in xylene (0.1 M solution) was stirred in sealed tube at 155 °C for 2 days and then the reaction mixture was concentrated. The residue was purified by column chromatography on silica gel (hexane/ethyl acetate = 6:1) to give compound **14** in 50% yield.

5.7.1. Ethyl 2-((6-methyl-2-oxo-2*H*-chromen-3-yl)methyl)-6-phenylhexanoate (14a)

^{1}H NMR ($CDCl_3$, 400 MHz) δ 7.44 (s, 1H), 7.38–7.15 (m, 8H), 4.03 (m, 2H), 2.88–2.74 (m, 3H), 2.60 (t, J = 7.6 Hz, 2H), 2.38 (s, 3H), 1.75–1.37 (m, 6H), 1.09 (q, J = 7.2 Hz, 3H); MS (ESI) m/z 415 (MNa^+).

5.7.2. Ethyl 2-(4-(benzyloxy)benzyl)-3-(6-methyl-2-oxo-2*H*-chromen-3-yl)propanoate (14b)

^{1}H NMR ($CDCl_3$, 400 MHz) δ 7.44–7.10 (m, 11H), 6.88 (d, J = 8.4 Hz, 2H), 5.02 (s, 2H), 3.94 (q, J = 7.2 Hz, 2H), 3.22–2.74 (m, 5H), 2.38 (s, 3H), 1.00 (t, J = 7.2 Hz, 3H); MS (ESI) m/z 457 (MH^+).

5.7.3. Ethyl 4-(4-(benzyloxy)phenyl)-2-((7-methyl-2-oxo-2*H*-chromen-3-yl)methyl)-butanoate (14i)

^{1}H NMR ($CDCl_3$, 400 MHz) δ 7.44–7.27 (m, 7H), 7.11–7.05 (m, 4H), 6.89 (d, J = 8.4 Hz, 2H), 5.04 (s, 2H), 4.06 (q, J = 7.2 Hz, 2H), 2.95–2.58 (m, 5H), 2.44 (s, 3H), 2.02–1.80 (m, 2H), 1.14 (t, J = 7.2 Hz, 3H); MS (ESI) m/z 493 (MNa^+).

5.8. General procedures for 16

Pd/C (10 wt %, 40.0 mg) was added to a solution of **15** (1.0 equiv) in EtOH (0.2 M solution). The mixture was stirred under H_2 atmosphere at room temperature for 5 h. The catalyst was removed by through pad of Celite and washed with EtOH. The solvent was evaporated in vacuo to give compound **16** in 80–90% yield.

5.8.1. Ethyl 2-(4-hydroxybenzyl)-3-(6-methyl-2-oxo-2*H*-chromen-3-yl)propanoate (16a)

^{1}H NMR ($CDCl_3$, 400 MHz) δ 7.47 (s, 1H), 7.29–7.05 (m, 3H), 7.06 (d, J = 8.4 Hz, 2H), 6.75 (d, J = 8.4 Hz, 2H), 5.65 (br, 1H), 3.96 (q, J = 7.2 Hz, 2H), 3.20–2.73 (m, 5H), 2.38 (s, 3H), 1.01 (t, J = 7.3 Hz, 3H).

5.8.2. Ethyl 4-(4-hydroxyphenyl)-2-((7-methyl-2-oxo-2*H*-chromen-3-yl)methyl)butanoate (16g)

^{1}H NMR ($CDCl_3$, 400 MHz) δ 7.45 (s, 1H), 7.27 (d, J = 7.6 Hz, 1H), 7.12 (s, 1H), 7.08–7.04 (m, 3H), 6.75 (d, J = 8.4 Hz, 2H), 4.81 (br, 1H), 4.07 (q, J = 7.2 Hz, 2H), 2.94–2.44 (m, 5H), 2.39 (s, 3H), 2.02–1.80 (m, 2H), 1.15 (t, J = 7.2 Hz, 3H); MS (ESI) m/z 403 (MNa^+).

5.8.3. Ethyl 2-((7-fluoro-2-oxo-2*H*-chromen-3-yl)methyl)-4-(4-hydroxyphenyl)butanoate (16h)

^{1}H NMR ($CDCl_3$, 400 MHz) δ 7.46 (s, 1H), 7.39 (dd, J = 8.4, 5.9 Hz, 1H), 7.05–6.97 (m, 4H), 6.76 (d, J = 8.4 Hz, 2H), 4.96 (br, 1H), 4.07 (q, J = 7.2 Hz, 2H), 2.93–2.58 (m, 5H), 1.99–1.77 (m, 2H), 1.16 (t, J = 7.2 Hz, 3H); MS (ESI) m/z 407 (MNa^+).

5.9. General procedures for 17

A mixture of **16** (1.0 equiv), 1-(2-chloroethyl)piperidine hydrochloride (1.5 equiv), NaI (1.5 equiv) and Cs_2CO_3 (3.0 equiv) in DMF (0.2 M solution for **16**) was stirred at 85 °C. After 6 h, the reaction mixture was concentrated. The residue was purified by column chromatography on silica gel (chloroform/methanol = 8:1) to give compound **17a–f** in 60–80% yield.

5.9.1. Ethyl 3-(6-methyl-2-oxo-2*H*-chromen-3-yl)-2-(4-(2-(piperidin-1-yl)ethoxy)benzyl)-propanoate (17a)

^{1}H NMR ($CDCl_3$, 400 MHz) δ 7.45 (s, 1H), 7.29–7.18 (m, 3H), 7.11 (d, J = 8.4 Hz, 2H), 6.78 (d, J = 8.4 Hz, 2H), 4.23 (t, J = 5.6 Hz, 2H), 3.96 (q, J = 7.2 Hz, 2H), 3.20–2.73 (m, 11H), 2.39 (s, 3H), 1.82–1.55 (m, 6H), 1.02 (t, J = 7.2 Hz, 3H).

5.9.2. Ethyl 4-(4-(2-(diethylamino)ethoxy)phenyl)-2-((7-methyl-2-oxo-2*H*-chromen-3-yl)methyl)butanoate (17i)

^{1}H NMR ($CDCl_3$, 400 MHz) δ 7.45 (s, 1H), 7.29 (d, J = 7.6, 1H), 7.11–7.05 (m, 4H), 6.82 (d, J = 8.4 Hz, 2H), 4.10–4.01 (m, 4H), 2.96–2.57 (m, 11H), 2.44 (s, 3H), 2.02–1.81 (m, 2H), 1.15 (t, J = 7.2 Hz, 3H), 1.07 (t, J = 7.2 Hz, 6H).

5.9.3. Ethyl 4-(4-(2-(diethylamino)ethoxy)phenyl)-2-((7-fluoro-2-oxo-2*H*-chromen-3-yl)methyl)butanoate (17j)

^{1}H NMR ($CDCl_3$, 400 MHz) δ 7.46 (s, 1H), 7.39 (dd, J = 8.6, 6.0 Hz, 1H), 7.09 (d, J = 8.6 Hz, 2H), 7.05–6.98 (m, 2H), 6.82 (d, J = 8.6 Hz, 2H), 4.10–4.02 (m, 4H), 2.92–2.58 (m, 11H), 2.06–1.81 (m, 2H), 1.08 (t, J = 7.2 Hz, 6H), 1.16 (t, J = 6.8 Hz, 3H).

5.9.4. Ethyl 4-(4-(2-(dimethylamino)ethoxy)phenyl)-2-((6-methyl-2-oxo-2*H*-chromen-3-yl)methyl)butanoate (17g)

60% NaH (52.6 mg, 1.31 mmol, 2.5 equiv) was added to a solution of **16** (200.0 mg, 0.53 mmol) in DMF (20 mL) at 0 °C. After 30 min, 2-chloro-*N*,*N*-dimethylethanamine hydrochloride (151.7 mg, 1.05 mmol, 2.0 equiv) was added and the reaction mixture was heated at 70 °C for 12 h. The mixture was poured into ice water and extracted with ethyl acetate. The organic layer was washed with brine, dried over anhydrous $MgSO_4$, filtered, and concentrated. The residue was purified by column chromatography on silica gel (chloroform/methanol = 10:1) to give compound **17g** (114.0 mg, 48%). ^{1}H NMR ($CDCl_3$, 400 MHz) δ 7.43 (s, 1H), 7.29–7.19 (m, 3H), 7.09 (d, J = 8.4 Hz, 2H), 6.84 (d, J = 8.4 Hz, 2H), 4.10–4.03 (m, 4H), 2.96–2.58 (m, 7H), 2.39 (s, 3H), 2.34 (s, 6H), 2.02–1.17 (m, 2H), 1.15 (t, J = 8.8 Hz, 3H); MS (ESI) m/z 474 (MNa^+).

5.10. General procedures for 15

NH_2OH in MeOH (1.76 M solution, 20 equiv) was added to a solution of **16** (1.0 equiv) in MeOH (0.25 M solution). The mixture was stirred at room temperature for 4 h and concentrated. The residue was purified by column chromatography on silica gel (hexane/ethyl acetate = 2:1) to give compound **15** in 10–30% yield.

5.10.1. 2-((6-Methyl-2-oxo-2*H*-chromen-3-yl)methyl)-6-phenylhexanoic acid hydroxyamide (15a)

^{1}H NMR (DMSO-d_6, 400 MHz) δ 10.39 (s, 1H), 8.67 (s, 1H), 7.63 (s, 1H), 7.41 (s, 1H), 7.37–7.12 (m, 7H), 2.60–2.34 (m, 5H), 2.34 (s, 3H), 1.56–1.22 (m, 6H); MS (FAB) m/z 380 (MH^+), HRMS (FAB) calcd for $C_{23}H_{25}NO_4(MH^+)$ 380.1862, found 380.1862.

5.10.2. *N*-Hydroxy-4-(4-hydroxyphenyl)-2-((6-methyl-2-oxo-2*H*-chromen-3-yl)methyl)butan-amide (15b)

^{1}H NMR (DMSO-d_6, 400 MHz) δ 10.45 (s, 1H), 8.74 (s, 1H), 7.64 (s, 1H), 7.41 (s, 1H), 7.36 (d, J = 8.4 Hz, 1H), 7.28 (d, J = 8.0 Hz, 1H), 6.94 (d, J = 7.7 Hz, 2H), 6.56 (d, J = 8.0 Hz, 2H), 2.59–2.61 (m, 2H), 2.37–2.41 (m, 3H), 2.35 (s, 3H), 1.74–1.78 (m, 1H), 1.57–1.61 (m, 1H); MS (FAB) *m/z* 368 (MH^+), HRMS (FAB) calcd for $C_{21}H_{21}NO_5(MH^+)$ 368.1498, found 368.1500.

5.10.3. 3-(6-Methyl-2-oxo-2*H*-chromen-3-yl)-2-(4-(2-(piperidin-1-yl)ethoxy)benzyl)propanoic acid hydroxyamide (15c)

^{1}H NMR (DMSO-d_6, 400 MHz) δ 10.37 (s, 1H), 8.46 (s, 1H), 7.65 (s, 1H), 7.41 (s, 1H), 7.37–7.35 (m, 2H), 7.08 (d, J = 8.4 Hz, 2H), 6.81 (d, J = 8.4 Hz, 2H), 3.99 (d, J = 5.6 Hz, 2H), 2.82–2.49 (m, 11H), 2.35 (s, 3H), 1.53–1.36 (m, 6H); MS (FAB) *m/z* 465 (MH^+), HRMS (FAB) calcd for $C_{27}H_{32}N_2O_5(MH^+)$ 465.2389, found 465.2390.

5.10.4. 3-(6-Methyl-2-oxo-2*H*-chromen-3-yl)-2-(3-(2-(piperidin-1-yl)ethoxy)benzyl)propanoic acid hydroxyamide (15d)

^{1}H NMR (DMSO-d_6, 400 MHz) δ 10.37 (s, 1H), 8.65 (s, 1H), 7.66 (s, 1H), 7.42–7.13 (m, 4H), 6.80–6.70 (m, 3H), 4.04 (t, J = 5.6 Hz, 2H), 3.58–1.23 (m, 17H), 2.35 (s, 3H); MS (FAB) *m/z* 481 (MH^+).

5.10.5. 2-((6-Methyl-2-oxo-2*H*-chromen-3-yl)methyl)-4-(4-(2-(piperidin-1-yl)ethoxy)phenyl)-butanoic acid hydroxyamide (15e)

^{1}H NMR (DMSO-d_6, 400 MHz) δ 10.46 (s, 1H), 8.72 (br, 1H), 7.64 (s, 1H), 7.41 (s, 1H), 7.37 (d, J = 8.4 Hz, 1H), 7.27 (d, J = 8.4 Hz, 1H), 7.06 (d, J = 8.8 Hz, 2H), 6.82 (d, J = 8.8 Hz, 2H), 4.00 (t, J = 6.0 Hz, 2H), 2.64–2.42 (m, 11H), 2.35 (s, 3H), 1.85–1.55 (m, 2H), 1.51–1.32 (m, 6H); MS (FAB) *m/z* 479 (MH^+), HRMS (FAB) calcd for $C_{28}H_{34}N_2O_5(MH^+)$ 479.2546, found 479.2546.

5.10.6. 2-((6-Methyl-2-oxo-2*H*-chromen-3-yl)methyl)-4-(3-(2-(piperidin-1-yl)ethoxy)phenyl)-butanoic acid hydroxyamide (15f)

^{1}H NMR (DMSO-d_6, 400 MHz) δ 10.49 (br, 1H), 8.32 (s, 1H), 7.66 (s, 1H), 7.47–6.90 (m, 7H), 4.02 (t, J = 4.9 Hz, 2H), 2.66–2.40 (m, 11H), 2.35 (s, 3H), 1.83–1.64 (m, 2H), 1.52–1.36 (m, 6H); MS (FAB) *m/z* 480 (MH^+), HRMS (FAB) calcd for $C_{28}H_{34}N_2O_5(MH^+)$ 479.2546, found 479.2546.

5.10.7. 2-((6-Methyl-2-oxo-2*H*-chromen-3-yl)methyl)-5-(4-(2-(piperidin-1-yl)ethoxy)phenyl)-pentanoic acid hydroxyamide (15g)

^{1}H NMR (DMSO-d_6, 400 MHz) δ 10.43 (s, 1H), 8.69 (s, 1H), 7.65 (s, 1H), 7.43 (s, 1H), 7.38 (d, J = 8.4 Hz, 1H), 7.28 (d, J = 8.4 Hz, 1H), 7.10 (d, J = 8.0 Hz, 2H), 6.86 (d, J = 8.0 Hz, 2H), 4.23–4.15 (m, 2H), 3.42–2.40 (m, 11H), 2.35 (s, 3H), 1.84–1.36 (m, 10H); MS (FAB) *m/z* 493 (MH^+), HRMS (FAB) calcd for $C_{29}H_{36}N_2O_5(MH^+)$ 493.2702, found 493.2702.

5.10.8. 2-((6-Methyl-2-oxo-2*H*-chromen-3-yl)methyl)-5-(3-(2-(piperidin-1-yl)ethoxy)phenyl)-pentanoic acid hydroxyamide (15h)

^{1}H NMR ($CDCl_3$, 400 MHz) δ 7.45 (s, 1H), 7.30–7.11 (m, 4H), 6.72 (d, J = 8.0 Hz, 1H), 6.68–6.65 (m, 2H), 5.40 (br, 1H), 4.09–4.01 (m, 2H), 2.94–2.71 (m, 3H), 2.59 (t, J = 7.2 Hz, 2H), 2.39 (s, 3H), 1.75–1.55 (m, 4H), 1.12 (t, 7.2 Hz, 3H); MS (FAB) *m/z* 493 (MH^+), HRMS (FAB) calcd for $C_{29}H_{36}N_2O_5(MH^+)$ 493.2702, found 493.2702.

5.10.9. 4-(4-(2-(Dimethylamino)ethoxy)phenyl)-2-((6-methyl-2-oxo-2*H*-chromen-3-yl)-methyl)butanoic acid hydroxyamide (15i)

^{1}H NMR (DMSO-d_6, 400 MHz) δ 10.43 (s, 1H), 8.71 (br, 1H), 7.61 (s, 1H), 7.38–7.23 (m, 3H), 7.03 (d, J = 8.4 Hz, 2H), 6.79 (d, J = 8.4 Hz, 2H), 3.97 (t, J = 6.0 Hz, 2H), 2.56–2.39 (m, 7H), 2.31 (s, 3H), 2.17 (s, 6H), 1.73–1.52 (m, 2H); MS (FAB) *m/z* 439 (MH^+), HRMS (FAB) calcd for $C_{25}H_{30}N_2O_5(MH^+)$ 439.2233, found 439.2236.

5.10.10. 4-(4-(2-(Diethylamino)ethoxy)phenyl)-2-((6-methyl-2-oxo-2*H*-chromen-3-yl)-methyl)-butanoic acid hydroxyamide (15j)

^{1}H NMR (DMSO-d_6, 400 MHz) δ 10.46 (s, 1H), 8.74 (s, 1H), 7.65 (s, 1H), 7.42 (s, 1H), 7.38 (d, J = 8.4 Hz, 1H), 7.28 (d, J = 8.4 Hz, 1H), 7.06 (d, J = 8.4 Hz, 2H), 6.82 (d, J = 8.4 Hz, 2H), 3.97 (t, J = 6.0 Hz, 2H), 2.77–2.42 (m, 11H), 2.35 (s, 3H), 1.80–1.60 (m, 2H), 0.97 (t, J = 7.2 Hz, 6H); MS (FAB) *m/z* 467 (MH^+), HRMS (FAB) calcd for $C_{27}H_{34}N_2O_5(MH^+)$ 467.2546, found 467.2547.

5.10.11. 4-(4-(2-(Diethylamino)ethoxy)phenyl)-2-((7-fluoro-2-oxo-2*H*-chromen-3-yl)methyl)-butanoic acid hydroxyamide hydrochloride (15k)

^{1}H NMR (DMSO-d_6, 400 MHz) δ 10.49 (s, 1H), 9.80 (br, 1H), 7.69 (s, 1H), 7.52 (d, J = 8.0 Hz, 1H), 7.21 (s, 1H), 7.17–7.12 (m, 3H), 6.90 (t, J = 5.2 Hz, 2H), 4.29 (t, J = 5.2 Hz, 2H), 3.60 (br, 1H), 3.50–3.21 (m, 6H), 2.59–2.44 (m, 5H), 2.40 (s, 3H), 1.80–1.59 (m, 2H), 1.23 (t, J = 7.2 Hz, 6H); MS (FAB) *m/z* 471 (MH^+), HRMS (FAB) calcd for $C_{26}H_{31}FN_2O_5(MH^+)$ 471.2295, found 471.2294.

5.10.12. 4-(4-(2-(Diethylamino)ethoxy)phenyl)-2-((7-methyl-2-oxo-2*H*-chromen-3-yl)methyl)-butanoic acid hydroxyamide hydrochloride (15l)

^{1}H NMR (DMSO-d_6, 400 MHz) δ 10.48 (s, 1H), 10.12 (s, 1H), 7.67 (s, 1H), 7.50 (d, J = 8.0 Hz, 1H), 7.20 (s, 1H), 7.14 (d, J = 8.0 Hz, 1H), 7.10 (d, J = 8.4 Hz, 2H), 6.88 (d, J = 8.4 Hz, 2H), 4.4 (br, 1H), 4.29–2.38 (m, 13H), 1.80–1.57 (m, 2H), 1.22 (t, J = 7.2 Hz, 6H); MS (FAB) *m/z* 467 (MH^+), HRMS calcd for $C_{27}H_{34}N_2O_5(MH^+)$ 467.2546, found 467.2549.

5.11. Biology

5.11.1. TACE, MMP-3, and MMP-9 enzyme inhibition assay

The enzymatic activity of human TACE (R&D Systems, Minneapolis, MN, USA) was determined at 25 °C with a synthetic fluorogenic substrate, Mca-Pro-Leu-Ala-Gln-Ala-Val-Dpa-Arg-Ser-Ser-Ser-Agr-NH_2 (Mca: [7-methoxycoumarin-4-yl] acetyl; Dpa: *N*-3-[2,4-dinitrophenyl]-L-2,3-diaminopropionyl, R&D Systems, Minneapolis, MN, USA). The enzymatic activities of MMP-3 and MMP-9 were determined with recombinant human version catalytic domains (Roche Applied Science, D-68298 Manheim, Germany) and a fluorogenic peptide substrate, Mca-Pro-Leu-Gly-Leu-Dpa-Ala-Arg-NH_2 (Sigma Chemical Co., PO Box 14508, St. Louis, MO 63178, USA). Fluorescence measurements were performed in a Perkin–Elmer Luminescence Spectrometer LS50B. Cleavage of internal quenched substrate liberates emission-active Mca product, causing an increase in fluorescence emission at 420 nM (the excitation wavelength is 324 nM). The rate of emission change is proportional to enzyme activity.

5.11.2. Cellular NO assay and TNF-α immunoassay

RAW264.7 cells were cultured with inhibitors for 24 h. NO_2^- accumulation was used as an indicator of NO production in the medium. The isolated supernatants were mixed with an equal volume of Griess reagent (1% sulfanilamide, 0.1% naphthylethylen-

ediamine dihydrochloride, and 2% phosphoric acid) and incubated at room temperature for 10 min. Nitrite production was determined by measuring absorbance at 540 nm versus a $NaNO_2$ standard curve. The concentration of TNF-α secreted in the culture supernatant of RAW264.7 cells was determined by ELISA, according to the manufacture's instruction (R&D Systems, Minneapolis, MN, USA).

5.12. Pharmacology and pharmacokinetics

5.12.1. In vivo TNF-α reproduction assay

To test the inhibitory activity of TNF-α reproduction, the level of TNF-α in blood of BALB/c mice (7–9 weeks, Japan SLC, Inc.) was measured. 10 μg/mouse of LPS (Sigma, L-2880) was intraperitoneally administrated into the mice to induce inflammation and mice had been starved for 24 h before use. Appropriate concentration of the compound (0.2 mg/mouse) was orally administrated thereto and lipopolysaccharide was further treated after 30 min. After 90 min, the serum was collected from the heart, and level of TNF-α in the isolated serum was determined by ELISA according to the manufacture's instruction (Biosource International, USA)

5.12.2. Carrageenan-induced paw edema test in rat

Sprague–Dawley rats (150 g, 5 weeks, SPF) were divided into four groups consisting of five rats each group: vehicle, 10 mg/kg of indomethacin, 30 mg/kg of **15l**, and 100 mg/kg of **15l**. Indomethacin was diluted with mixture solution of DMSO, Tween 80, and H_2O (1:4:95) to use as positive control group and **15l** was diluted with mixture solution of ethanol, PEG (polyethylene glycol) 400, and H_2O (5:20:75) to use as a test group. After 30 min, 100 μL of 2% carrageenan (Sigma, c-1013) solution was injected into inner rat to induce edema. The thickness of ankle was measured by bernier's caliper to determine the degree of the edema after 6 and 24 h. The thickness ratio of ankle (%) = [(maximum thickness of rat paw edema) − (the thickness of pre-treated rat paw edema)]/(the thickness of pre-treated rat paw edema) × 100%.

5.12.3. Human liver microsomal stability test

Compound **15l** or DPC-333 (1 μM, 40 μL), Human liver microsome (BD gentest, 20 μL, final concn 1 mg/mL) and $MgCl_2$ (40 μL) was added to potassium phosphate buffer. The solution was incubated for 5 min at 37 °C and added β-NADPH (Sigma, 100 μL, final concn 1 mM). Aliquots of 100 μL are removed from the incubations at varying time intervals; 0, 15, 45, and 80 min. The reactions are terminated by the addition of ice cold acetonitrile 200 μL and internal standard 100 μL (carbamazepine, 1000 ng/mL). The samples were centrifuged at 3000 rpm for 10 min and analysis by LC/MS/MS.

5.12.4. Rat pharmacokinetic (PK) study

Male SD rats were acclimated to the testing facility in a temperature and humidity controlled condition for approximately a week prior to the study. Male SD rats (10-week old, 285–305 g) were cannulated in the right jugular vein. **15l** dissolved saline were dosed iv or po in SD rats. About 300 μL of blood samples were collected in BD microtainer plasma separator tubes at selected times through the jugular vein cannula over 24 h post-dosing. Blood samples were centrifuged at 3000 rpm for 10 min and stored in a freezer until analyzed. Plasma samples were prepared for analysis by the following protein precipitation method. One hundred microliters of the plasma samples were transferred to a 96-well cluster tube plate. Three volumes of acetonitrile containing carbamazepine (IS) were added and the resulting mixture was vortexed for 5 min on a multi-tube vortexer. The 96-well cluster tube plate was then centrifuged at 12,000 rpm for 10 min and the supernatant was analyzed for quantitation of **15l**. Sample analysis was performed by API2000 LC/MS/MS system in a positive MRM mode (column: Waters Xterra MS C18 (2.1 × 50 mm, 3.5 μm); mobile phase: acetonitrile/DI water/0.1% formic acid; ion source: turbo ion spray). Analytical data were processed using Analyst™ 1.4.1. (Applied Biosystems, Concord, Canada). Pharmacokinetic parameters were obtained by non-compartmental analysis of the plasma concentration–time profiles using PK Solution 2.0 (Summit Research Services, Montrose, CO, USA).

Acknowledgments

This research was supported by National Research Foundation (2009-0092966), Korean Research WCU grant (R31-2008-000-10086-0) and the Brain Korea 21 project, the Republic of Korea.

Supplementary data

Supplementary data associated with this article can be found, in the online version, at doi:10.1016/j.bmc.2010.10.006. These data include MOL files and InChiKeys of the most important compounds described in this article.

References and notes

1. Tracey, K. J.; Cerami, A. *Annu. Rev. Med.* **1994**, *45*, 491.
2. Goldfeld, A. E.; Strominger, J. L.; Doyle, C. *J. Exp. Med.* **1991**, *174*, 73.
3. Le, G. T.; Abbenante, G. *Curr. Med. Chem.* **2005**, *12*, 2963.
4. Newton, R. C.; Decicco, C. P. *J. Med. Chem.* **1999**, *42*, 2295.
5. Hotamisligil, G. S.; Arner, P.; Caro, J. F.; Atkinson, R. L.; Spiegelman, B. M. *J. Clin. Invest.* **1995**, *95*, 2409.
6. Selmaj, K.; Raine, C. S.; Cannella, B.; Brosnan, C. F. *J. Clin. Invest.* **1991**, *87*, 949.
7. Rus, H. G.; Niculescu, F.; Vlaicu, R. *Atherosclerosis* **1991**, *89*, 247.
8. Lovering, F.; Zhang, Y. *Curr. Drug Targets CNS Neurol. Disord.* **2005**, *4*, 161.
9. Moreland, L. W.; Baumgartner, S. W.; Schiff, M. H.; Tindall, E. A.; Fleischmann, R. M.; Weaver, A. L.; Ettlinger, R. E.; Cohen, S.; Koopman, W. J.; Mohler, K.; Widmer, M. B.; Blosch, C. M. *N. Eng. J. Med.* **1997**, *337*, 141.
10. Lipsky, P. E.; van der Heijde, D. M.; St Clair, E. W.; Furst, D. E.; Breedveld, F. C.; Kalden, J. R.; Smolen, J. S.; Weisman, M.; Emery, P.; Feldmann, M.; Harriman, G. R.; Maini, R. N. *N. Eng. J. Med.* **2000**, *343*, 1594.
11. Machold, K. P.; Smolen, J. S. *Expert Opin. Biol. Ther.* **2003**, *3*, 351.
12. Moss, M. L.; Sklair-Tavron, L.; Nudelman, R. *Nat. Clin. Pract. Rheumatol.* **2008**, *4*, 300.
13. Nelson, F. C.; Zask, A. *Expert Opin. Invest. Drugs* **1999**, *8*, 383.
14. Wasserman, Z. R.; Duan, J. J.; Voss, M. E.; Xue, C. B.; Cherney, R. J.; Nelson, D. J.; Hardman, K. D.; Decicco, C. P. *Chem. Biol.* **2003**, *10*, 215.
15. Shaw, T.; Nixon, J. S.; Bottomley, K. M. *Expert Opin. Invest. Drugs* **2000**, *9*, 1469.
16. Aranapakam, V.; Davis, J. M.; Grosu, G. T.; Baker, J.; Ellingboe, J.; Zask, A.; Levin, J. I.; Sandanayaka, V. P.; Du, M.; Skotnicki, J. S.; DiJoseph, J. F.; Sung, A.; Sharr, M. A.; Killar, L. M.; Walter, T.; Jin, G.; Cowling, R.; Tillett, J.; Zhao, W.; McDevitt, J.; Xu, Z. B. *J. Med. Chem.* **2003**, *46*, 2376.
17. Park, S. K.; Han, S. B.; Lee, K.; Lee, H. J.; Kho, Y. H.; Chun, H.; Choi, Y.; Yang, J. Y.; Yoon, Y. D.; Lee, C. W.; Kim, H. M.; Choi, H. M.; Tae, H. S.; Lee, H. Y.; Nam, K. Y.; Han, G. *Biochem. Biophys. Res. Commun.* **2006**, *341*, 627.
18. Chun, K.; Park, S. K.; Kim, H. M.; Choi, Y.; Kim, M. H.; Park, C. H.; Joe, B. Y.; Chun, T. G.; Choi, H. M.; Lee, H. Y.; Hong, S. H.; Kim, M. S.; Nam, K. Y.; Han, G. *Bioorg. Med. Chem.* **2008**, *16*, 530.
19. Hin, B.; Majer, P.; Tsukamoto, T. *J. Org. Chem.* **2002**, *67*, 7365.
20. Duan, J. J.; Chen, L.; Wasserman, Z. R.; Lu, Z.; Liu, R. Q.; Covington, M. B.; Qian, M.; Hardman, K. D.; Magolda, R. L.; Newton, R. C.; Christ, D. D.; Wexler, R. R.; Decicco, C. P. *J. Med. Chem.* **2002**, *45*, 4954.
21. Venkatachalam, C. M.; Jiang, X.; Oldfield, T.; Waldman, M. *J. Mol. Graphics Modell.* **2003**, *21*, 289.
22. Mazzola, R. D., Jr.; Zhu, Z.; Sinning, L.; McKittrick, B.; Lavey, B.; Spitler, J.; Kozlowski, J.; Neng-Yang, S.; Zhou, G.; Guo, Z.; Orth, P.; Madison, V.; Sun, J.; Lundell, D.; Niu, X. *Bioorg. Med. Chem. Lett.* **2008**, *18*, 5809.
23. Natchus, M. G.; Bookland, R. G.; De, B.; Almstead, N. G.; Pikul, S.; Janusz, M. J.; Heitmeyer, S. A.; Hookfin, E. B.; Hsieh, L. C.; Dowty, M. E.; Dietsch, C. R.; Patel, V. S.; Garver, S. M.; Gu, F.; Pokross, M. E.; Mieling, G. E.; Baker, T. R.; Foltz, D. J.; Peng, S. X.; Bornes, D. M.; Strojnowski, M. J.; Taiwo, Y. O. *J. Med. Chem.* **2000**, *43*, 4948.